Domain structure of epitaxial $Bi_4Ti_3O_{12}$ thin films grown on (001) $SrTiO_3$ substrates

X. Q. Pan[a] and J. C. Jiang
Department of Materials Science and Engineering, The University of Michigan, Ann Arbor, Michigan 48109-2136

C. D. Theis and D. G. Schlom
Department of Materials Science and Engineering, The Pennsylvania State University, University Park, Pennsylvania 16803-6602

(Received 30 April 2003; accepted 22 July 2003)

The domain structure of epitaxial (001) $Bi_4Ti_3O_{12}$ thin films grown on (001) $SrTiO_3$ substrates by reactive molecular beam epitaxy was studied using transmission electron microscopy. It was found that the $Bi_4Ti_3O_{12}$ thin films contain randomly distributed rotation domains of two different types, which are related by a 90° rotation around the *c* axis of $Bi_4Ti_3O_{12}$. These domains result from the difference in crystallographic symmetry between the $Bi_4Ti_3O_{12}$ (001) plane and the $SrTiO_3$ (001) surface. Moreover, out-of-phase boundaries were frequently observed in the epitaxial $Bi_4Ti_3O_{12}$ films. Detailed quantitative high-resolution transmission electron microscopy studies showed that the growth of epitaxial $Bi_4Ti_3O_{12}$ film on the $SrTiO_3$ (001) surface begins with the energetically favorable central TiO_2 layer in the middle of the triple perovskite block within $Bi_4Ti_3O_{12}$. As a result, a number of out-of-phase domain boundaries are formed at the atomic steps on the substrate surface. These studies suggest that $Bi_4Ti_3O_{12}$ films grow on (001) $SrTiO_3$ substrates through two-dimensional island growth mechanism, where individual domains nucleate with random orientations of their polar *a* axis along either [110] or $[1\bar{1}0]$ direction of $SrTiO_3$. © *2003 American Institute of Physics.* [DOI: 10.1063/1.1611277]

Bismuth titanate ($Bi_4Ti_3O_{12}$) is a member of the layered Aurivillius phase perovskite ferroelectrics and has a Curie temperature of 675 °C. In its ferroelectric state, $Bi_4Ti_3O_{12}$ is monoclinic. Its spontaneous polarization vector lies in the $a-c$ plane, with a component of 49 $\mu C/cm^2$ along the *a* axis and 4 $\mu C/cm^2$ along the *c* axis.[1] $Bi_4Ti_3O_{12}$ is an attractive material for use in nonvolatile memories[2,3] since it and other Aurivillius phases exhibit excellent fatigue resistance during repeated polarization reversals with electrical field.[4,5] Furthermore, its layered perovskite structure makes it feasible to grow lattice-matched heterostructures on various substrates by different thin film growth methods.[6–12] X-ray diffraction has been the main technique applied to structurally characterize epitaxial $Bi_4Ti_3O_{12}$ thin films. $Bi_4Ti_3O_{12}$ thin films grown on the (001) $SrTiO_3$ substrate were reported to be oriented with their *c* axis normal to the substrate surface.[7,10–12] However, little work has been done to study the microstructure and ferroelectric domain configurations of epitaxial $Bi_4Ti_3O_{12}$ thin films.[13,14] The components of spontaneous polarization along the *a* and *c* directions of $Bi_4Ti_3O_{12}$ can be independently reversed with an electrical field, resulting in several different domains and domain wall configurations.[15] All these configurations, which will influence the ferroelectric properties of thin films, have not been distinguished by x-ray diffraction in thin films. In this letter, we report the direct observations of ferroelectric domain configurations and antiphase boundaries in an epitaxial $Bi_4Ti_3O_{12}$ thin film grown on $SrTiO_3$ using transmission electron microscopy (TEM). $Bi_4Ti_3O_{12}$ has a commensurately modulated monoclinic layer-perovskite structure with space group $B1a1$ and lattice parameters $a=5.450$ Å, $b=5.4059$ Å, $c=32.832$ Å, and $\beta=90.00°$.[16] It consists of double BiO layers interleaved with $Bi_2Ti_3O_{10}$ perovskite layers. The TiO_6 octahedra are tilted about the three axes and the Bi and Ti atoms are displaced from the corresponding *A* and *B* sites in its ideal cubic perovskite ABO_3 structure. $SrTiO_3$ has a cubic perovskite structure with the space group of $Pm\bar{3}m$ and the lattice constant of $a=3.905$ Å.[17]

Epitaxial $Bi_4Ti_3O_{12}$ films were grown on (001) $SrTiO_3$ substrates by reactive molecular beam epitaxy at a substrate temperature of ~650 °C. The details of film growth are given elsewhere.[12] High-resolution transmission electron microscopy (HRTEM) studies were conducted with a JEOL 4000EX electron microscope with a point-to-point resolution of 0.17 nm.

Figure 1(a) is a dark-field image of a cross-sectional sample. Figures 1(b) and 1(c) are selected-area electron diffraction (SAED) patterns taken respectively from the bright and dark regions in Fig. 1(a) with the electron beam aligned parallel to the [110] axis of $SrTiO_3$ substrate. Figure 1(a) was formed using the reflection of $Bi_4Ti_3O_{12}$ which is marked by a circle in Fig. 1(b). Figure 1(b) corresponds to the [100] diffraction pattern, while Fig. 1(c) is the [010] diffraction pattern of $Bi_4Ti_3O_{12}$. The [110] zone axis diffraction pattern of the $SrTiO_3$ substrate also occurs in Fig. 1(b) and its reflection spots are marked by arrowheads. The systematic absence of reflections in Figs. 1(b) and 1(c) is consistent with the crystal symmetries of $Bi_4Ti_3O_{12}$, where there exist *B* center (resulting in the absence of *hkl* reflections when $h+l$ is odd) and a glide plane perpendicular to the *b* axis (resulting in the absence of $h0l$ reflections when *h* is odd). These results reveal that the $Bi_4Ti_3O_{12}$ film grows on the (001) $SrTiO_3$ substrate along the [001] direction, consisting

[a]Electronic mail: panx@umich.edu

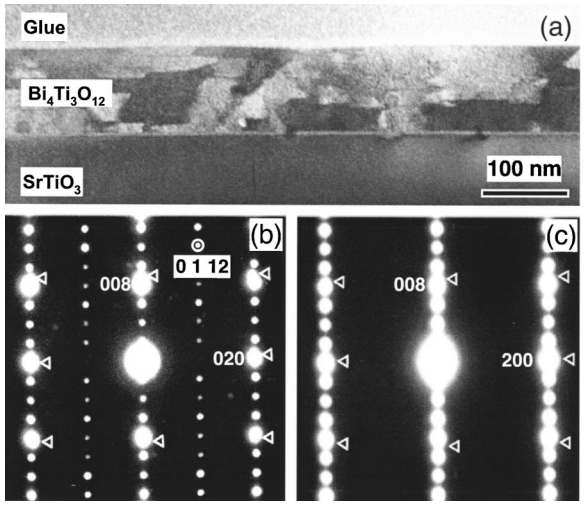

FIG. 1. (a) Dark-field image formed by the 0 1 12 reflection of $Bi_4Ti_3O_{12}$ showing two types of domain structures (bright and dark regions). The electron diffraction patterns of bright and dark regions are shown in (b) and (c), respectively.

of two different orientation domains: (I) $Bi_4Ti_3O_{12}$ (001) [100]//$SrTiO_3$ (001) [110]: (II) $Bi_4Ti_3O_{12}$ (001) [010] // $SrTiO_3$ (001) [110]. The two domain types differ by a 90° rotation along their [001] direction, i.e., the growth direction. It should be pointed out that there may exist other two types of rotation domains resulting from a rotation of the type I and type II domains by a 180° rotation around the [001] axis of $Bi_4Ti_3O_{12}$. The 180° domains cannot be distinguished in electron diffraction contrast images, but, the corresponding domain walls are visible, as shown by some fine fringes seen in Fig. 2(b).

Figure 2(a) shows a SAED pattern taken from a plan-view specimen of the same film as for Fig. 1. As pointed out previously, $hk0$ reflections with $h=$ odd are forbidden due to the crystallographic symmetry of $Bi_4Ti_3O_{12}$ [Fig. 1(c)]. The diffraction spots seen at these positions in Fig. 2(a) result from the superposition of two [001] patterns of $Bi_4Ti_3O_{12}$ that are rotated with respect to each other by 90° around their zone axis [001]. This is clearly seen in the cross-section dark-field image in Fig. 1(a). Moreover, the diffraction spots at $2m+1\ 2n+1\ 0$, where m and n are integers, are caused by the double diffraction of electron beam on passing through two overlapped domains. Figure 2(b) is the dark-field image obtained using the 210 weak reflection marked by an arrowhead and letter V in Fig. 2(a). The type I domains appear bright in Fig. 2(b), while the type II domains appear dark. Our TEM studies indicate that the rotation domains have a mean size of about 50 nm and are randomly distributed in the film. Both types of domains have equal volume fraction and have an elongation along the [100] and [010] directions, resulting from the structural anisotropy.

A number of translation domain walls exist, which appear as dark or bright fringes in the weak beam dark-field images in Fig. 2(b). The domains on both sides of the boundary have the same crystallographic orientations, but are shifted with respect to each other by a fraction of the lattice translation vectors of $Bi_4Ti_3O_{12}$. Figure 3(a) is the Bragg-filtered HRTEM image of an antiphase boundary observed in the same plane-view specimen as for Fig. 2. The two domains are shifted with respect to each other by $\frac{1}{2}b$

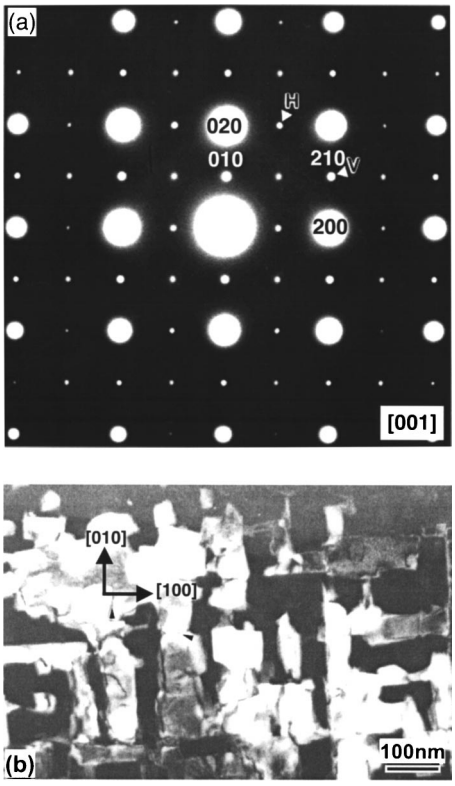

FIG. 2. (a) Electron diffraction pattern taken from a plan-view specimen. (b) Dark-field image formed by the 210 weak reflections marked by an arrowhead and letter V in (a). Spot indicated by an arrowhead and the letter H is the 210 reflection of the domain with 90° rotation.

along the [010] direction. Figure 3(b) shows the existence of out-of-phase boundaries observed in the same cross-sectional specimen as for Fig. 1. It is noted that two domain boundaries indicated by dashed lines originate from the film/substrate interface. Each boundary is associated with an atomic step on the substrate surface as indicated by the arrowheads. As seen in Fig. 3(b), the $SrTiO_3$ substrate surface is located at the same level both in the left side of step L and in the right side of step R, but is lowered by one unit cell height between the two steps.

To understand the formation mechanism of the out-of-phase boundaries observed, one has to consider the epitaxial growth mechanism of $Bi_4Ti_3O_{12}$. The (001) $SrTiO_3$ substrate was etched with a buffered-HF solution, exposing the TiO_2-terminated surface.[18] After annealing in high vacuum at the growth temperature (~650 °C) prior to growth, the atomic steps existing on the $SrTiO_3$ (001) surface mainly have a height of one unit cell.[19] Quantitative HRTEM studies of epitaxial $Bi_4Ti_3O_{12}$ thin films with different growth initiation sequences have revealed that the growth of $Bi_4Ti_3O_{12}$ thin films always begins with the central TiO_2 layer in the middle of the triple perovskite block within $Bi_4Ti_3O_{12}$ [Fig. 4(a)], which is shared by both the $Bi_4Ti_3O_{12}$ film and the $SrTiO_3$ substrate.[20] When an atomic step with one unit cell height exists on the TiO_2-terminated $SrTiO_3$ (001) surface, as schematically shown in Fig. 4(b), the growth of $Bi_4Ti_3O_{12}$ film with the same TiO_2 layer on both sides of the step will result in an out-of-phase boundary originating from the surface step of $SrTiO_3$.

It should be noted that there exist two central TiO_2 layers in each unit cell of $Bi_4Ti_3O_{12}$, as indicated by $M1$ and

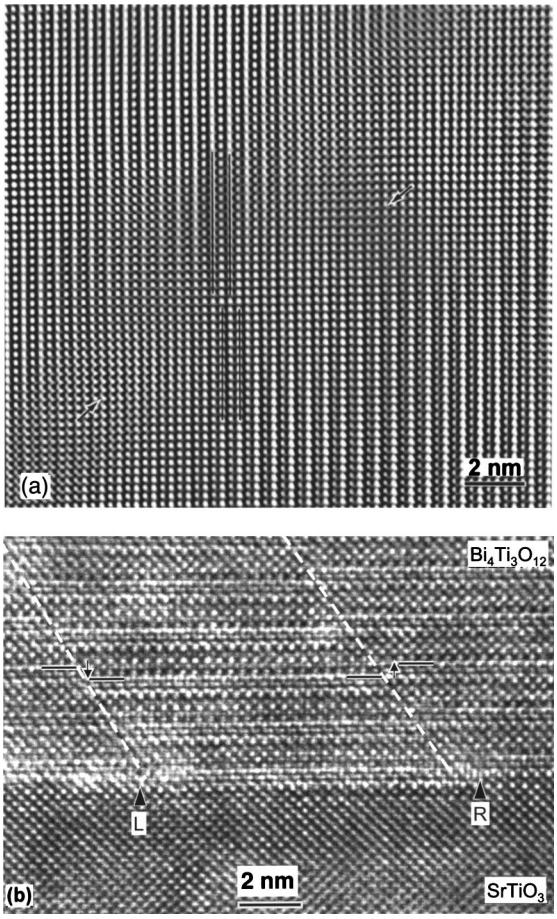

FIG. 3. (a) Fourier-filtered plan-view HRTEM image showing the atomic configuration of an antiphase boundary. (b) Cross-section HRTEM image showing the existence of out-of-phase boundaries associated with atomic steps on the substrate surface.

$M2$ in Fig. 4(a). The distance between $M1$ and $M2$ is $\frac{1}{2}c$. The atomic configuration in both layers are the same, but the atom positions in one layer are shifted with respect to the other by $\frac{1}{2}b$ due to the B centering of the $Bi_4Ti_3O_{12}$ structure. When $Bi_4Ti_3O_{12}$ initially grows with the $M1$ layer in one region and with the $M2$ layer in the other region on an *atomically smooth* substrate, the merging of these two regions (domains) will result in an out-of-phase boundary. In addition to the displacement of $\frac{1}{2}c$, there is also a displacement of $\frac{1}{2}b$ in the $a-b$ plane, resulting from the relative position of the $M1$ and $M2$ planes in the $Bi_4Ti_3O_{12}$ lattice. Therefore, the total displacement vector of this boundary is $\frac{1}{2}(b+c)$ and the boundary corresponds to antiphase boundary.

In conclusion, the epitaxial $Bi_4Ti_3O_{12}$ thin films grow along the c axis and consist of randomly distributed rotation domains (twins) of two different types, which differ by a 90° rotation around the c axis. The existence of these rotation domains is due to the difference in crystal symmetry between the film and the substrate: twofold symmetry in the (001) plane of $Bi_4Ti_3O_{12}$ and fourfold symmetry on the $SrTiO_3$ (001) surface. Furthermore, out-of-phase boundaries were frequently observed in $Bi_4Ti_3O_{12}$ films. Detailed HRTEM studies revealed that these boundaries can arise due to the existence of many atomic steps on the substrate surface.

The authors gratefully acknowledge the financial support of the National Science Foundation DMR through Grant No. 9875405, (CAREER X.Q.P.) DMR/IMR through Grant No. 9704175, and the Department of Energy through Grant No. DE-FG02-97ER45638 (D.G.S.).

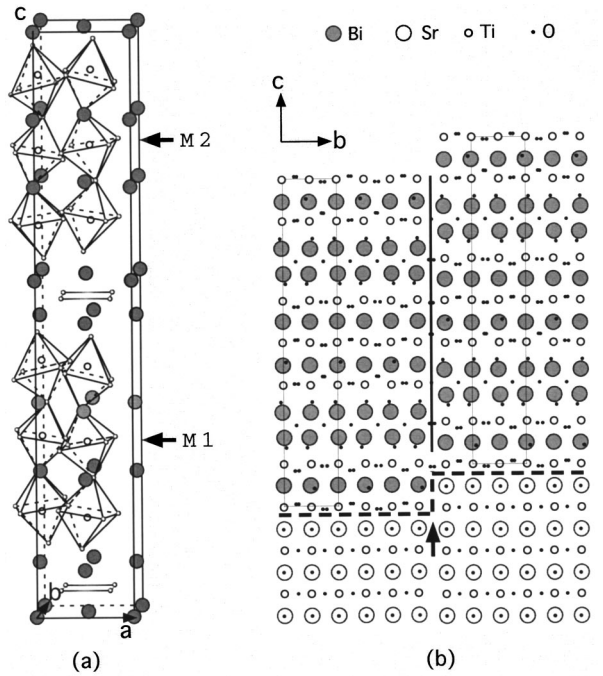

FIG. 4. (a) Schematic illustration of the crystal structure of $Bi_4Ti_3O_{12}$. (b) Schematic illustration of the atomic structure and formation mechanism of an out-of-phase boundary due to the existence of an atomic step on the substrate surface.

[1] S. E. Cummins and L. E. Cross, J. Appl. Phys. **39**, 2268 (1967).
[2] S. Y. Wu, W. J. Takei, and M. H. Francombe, Ferroelectrics **10**, 209 (1976).
[3] J. F. Scott and C. A. Paz de Araujo, Science **246**, 1400 (1989).
[4] P. C. Joshi and S. B. Krupanidhi, Appl. Phys. Lett. **62**, 1928 (1993).
[5] C. A-Paz de araujo, J. D. Cuchlaro, L. D. Mcmillan, M. C. Scott, and J. F. Scott, Nature (London) **374**, 627 (1995).
[6] W. J. Takei, N. P. Formigoni, and M. H. Francombe, Appl. Phys. Lett. **15**, 256 (1969).
[7] R. Ramesh, A. Inam, W. K. Chan, B. Wilkens, K. Myers, K. Remschnig, D. L. Hart, and J. M. Tarascon, Science **252**, 944 (1991); R. Ramesh, K. Luther, B. Wilkens, D. L. Hart, E. Wang, J. M. Tarascon, X. D. Wu, and T. Venkatesan, Appl. Phys. Lett. **57**, 1505 (1990).
[8] H. Buhay, S. Sinharoy, W. H. Kasner, M. H. Francombe, D. R. Lampe, and E. Stepke, Appl. Phys. Lett. **58**, 1505 (1990).
[9] N. Maffei and S. B. Krupanidhi, Appl. Phys. Lett. **60**, 781 (1992).
[10] W. Jo, G.-C. Yi, T. W. Noh, D.-K. Ko, Y. S. Cho, and S.-I. Kwun, Appl. Phys. Lett. **61**, 1516 (1992); W. Jo, H.-J. Cho, T. W. Noh, B. I. Kim, D.-Y. Kim, Z. G. Khim, and S.-I. Kwun, *ibid.* **63**, 2198 (1992).
[11] S. Choopun, T. Matsumoto, and T. Kawai, Appl. Phys. Lett. **67**, 1072 (1995).
[12] C. D. Theis, J. Yeh, D. G. Schlom, M. E. Hawley, G. W. Brown, J. C. Jiang, and X. Q. Pan, Appl. Phys. Lett. **72**, 2817 (1998).
[13] Y. Barad, J. Lettieri, C. D. Theis, D. G. Schlom, V. Gopalan, J. C. Jiang, and X. Q. Pan, J. Appl. Phys. **89**, 1387 (2001).
[14] T. Watanabe, H. Funakubo, K. Saito, T. Suzuki, M. Fujimoto, M. Osada, Y. Noguchi, and M. Miyayama, Appl. Phys. Lett. **81**, 1660 (2002).
[15] S. E. Cummins and L. E. Cross, J. Appl. Phys. **39**, 2268 (1968).
[16] A. D. Rae, J. G. Thompson, R. L. Withers, and A. C. Willis, Acta Crystallogr., Sect. B: Struct. Sci. **B46**, 474 (1990).
[17] W. Bensch, H. W. Schmalle, and A. Reller, Solid State Ionics **43**, 171 (1990).
[18] M. Kawasaki, K. Takahashi, T. Maeda, R. Tsuchiya, M. Shinohara, O. Ishiyama, T. Yonezawa, M. Yoshimoto, and H. Koinuma, Science **266**, 1540 (1994).
[19] C. D. Theis, J. Yeh, D. G. Schlom, M. E. Hawley, and G. W. Brown, Mater. Sci. Eng., B **56**, 228 (1998).
[20] J. C. Jiang, X. Q. Pan, and D. G. Schlom (unpublished).